Signal simulation under the bias rail in n⁺-in-p pixel sensor before and after irradiation

Y. Unno[a], R. Hori[a],
[a]KEK, IPNS, 1-1 Oho, Tsukuba, Ibaraki 305-0801, Japan

Abstract -- We have developed novel radiation-tolerant n⁺-in-p pixel sensors with biasing network from the outer bias ring to individual pixels. The network is to provide the reverse bias voltage to individual pixels. The biasing network enables to verify the high voltage operation of individual pixels for identifying the sensors having defective pixels, e.g. having the microdischarge at a lower bias voltage. The pixel sensors showed little efficiency loss, initially, before irradiation. After irradiation, the same device/ geometry showed efficiency loss, especially under the bias rail, noticeably. In order to understand the underlying physics, we have developed a Monte Carlo signal simulation program with the standard procedures of Ramo's potential and drifting carriers. We have imported electric fields and the weighting potentials in high precision from TCAD calculations and evaluated the charges lost to the bias rail with and without radiation damage. The comparison has confirmed the efficiency loss quantitatively and the insight into the underlying physics.

- Bias rail structure in n⁺-in-p pixel sensor Ref.[3]

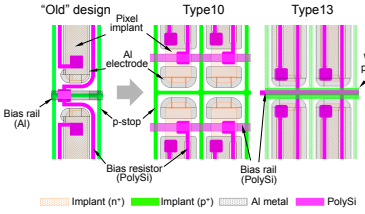

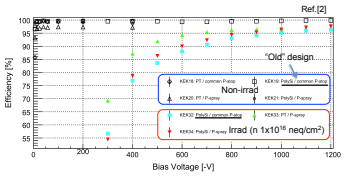

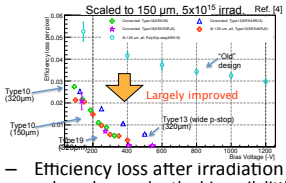

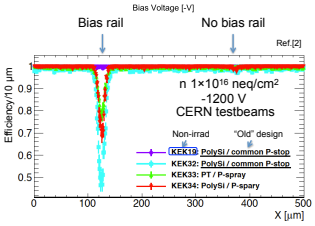

  - Efficiency loss after irradiation
    - large loss under the bias rail; little loss without the rail
    - ~3%/pixel (irrad); <~1%/pixel (non-irrad.)

- TCAD Simulation Ref.[5] for (a) Electric and (b) Weighting fields Ref.[3]
  - Geometry: vicinity of bias rail
    - p-type bulk, n⁺ readout, thickness 150 μm
  - Radiation damage approximation:
    - Increase of acceptor-like state ← Effective doping concentration
    - Increase of interface charge ← Fixed oxide charge
  - Non irrad. condition
    - N_{eff}=4.7×10¹² cm⁻³, V_{FD} ~40 V
    - Fixed Oxide Charge =1×10¹⁰ cm⁻²
  - Irrad. condition
    - N_{eff}=1.5×10¹³ cm⁻³, V_{FD} ~430 V
    - Fixed Oxide Charge =1×10¹² cm⁻²

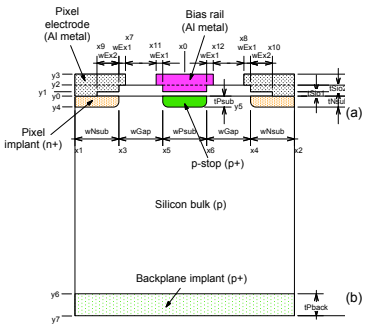

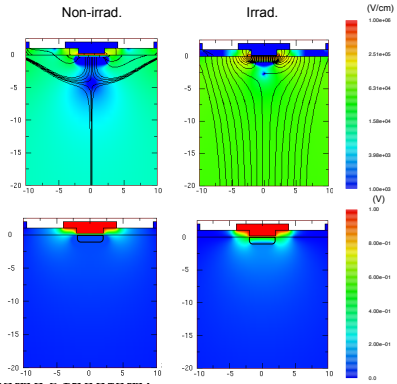

- Induced charge to the bias rail (Ramo's theorem)
  - A mobile charge in the presence of any number of grounded electrodes, the induced charge Q_A at an electrode A is

$$Q_A = q \cdot V_{qA}$$

    - where q is the charge in a position, V_{qA} **the "weighting potential"** of the electrode A at the position of q.
  - In a finite time, with a fast readout circuitry, **instantaneous induced current, i_A, is the gradient of V_{qA} along the moving direction times the drift velocity**.

$$i_A = q\frac{dV_{qA}}{dt} = q\left(\frac{\partial V_{qA}}{\partial x}\frac{dx}{dt}\right) = q \cdot \vec{v_x} \cdot \frac{\partial V_{qA}}{\partial x}$$

$$\vec{v_x} = \mu \vec{E_x} = \mu \frac{\partial V_x}{\partial x}$$

  - Although the final answer shall be obtained after integrating the current, we can have physics insight, **qualitatively**, from

$$E_x,\ v_x,\ V_{qA}$$

- Signal simulation
  - Using the simulation package Ref.[6] with various updates

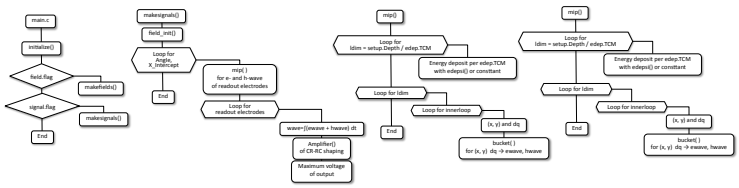

- Drift velocities Ref.[7], Energy deposition

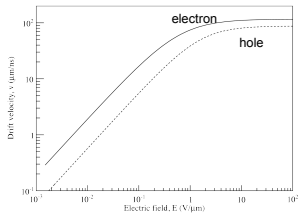

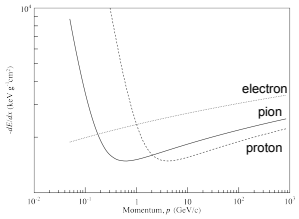

- Electric fields and Weighting potentials from TCAD
  - Non-irrad
  - Irrad.

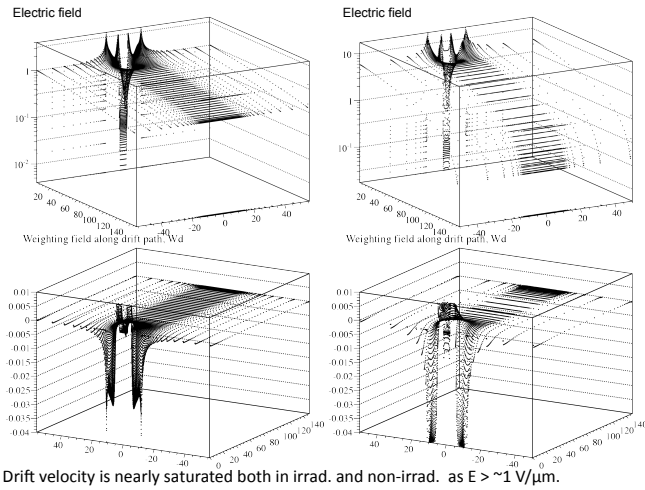

  - Drift velocity is nearly saturated both in irrad. and non-irrad. as E > ~1 V/μm.

- Induced currents (e, h) and charges (integrated, after pulse-shaping)

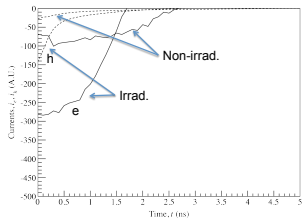

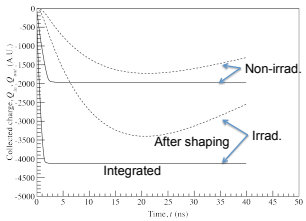

  - Bipolar nature of the current is not in the plot as the drift was cut off near the surface (at 3 μm) due to programming issue.

- Max. charges after pulse-shaping vs incident x position

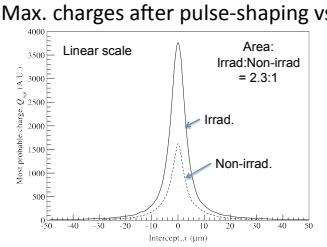

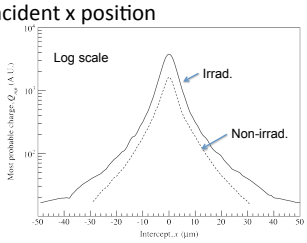

- Summary
  - Charges lost to the bias rail is approximately 2.3 times in irrad. than in non-irrad. This explains the difference of efficiency loss in the irrad. and non-irrad, **quantitatively**.
  - The difference in intensity of charges lost is due to the difference in the convolution of the intensity of the weighting potential and the drift path as the drift velocity is nearly saturated in both irrad and non-irrad.

- References

[1] Y. Unno et al., Nucl. Instr. Meth. A650 (2011) 129-135; Y. Unno et al., Nucl. Instr. Meth. A699 (2013) 72-77
[2] K. Motohashi et al. , Nucl. Instr. Meth. A765 (2014) 125-129
[3] Y. Unno et al., Nucl. Instr. Meth. A831 (2016) 122-132
[4] K. Nakamura et al., 2015 JINST 10 C06008; K. Kimura et al., Nucl. Instr. Meth. A831 (2016) 140-146
[5] ENEXSS 5.5, developed by SELETE in Japan
[6] J. Leslie et al., IEEE Trans. Nucl. Scie. 40 (1993) 206-208
[7] R.S. Muller, T.I. Kamins, Device Electronics for Integrated Circuits, ISBN-978-0-471-59398-0, John Wileys & Sons, Inc.